URSI AP-RASC, Sydney, Australia, 17 – 22 August 2025

Assessing the Impact of Ingesting Oblique Ionograms on Specifying the Ionosphere

Camella Nasr[(1)], Joe Hughes[(1,2)], Anastasia Newheart[(1)], Ian Collett[(1)], Elijah Vance[(1)], Ryan Kelly[(1)], Jeffrey Steward[(1)], Tristan Clark[(1)], Shawn Madison[(1)], Ryan Blay[(1)], Connor Johnstone[(1)]
(1) Orion Space Solutions, Louisville CO, USA
(2) Northwest Research Associates, Boulder CO, USA

Abstract

Oblique ionograms (OIs) are measurements of the group path delay as a function of frequency for a High Frequency link where the transmitter is far from the receiver. They are more complex than vertical ionograms (VIs), as the ray travels along different paths for each frequency. In this work, we use a simple approximation to transform an OI into the equivalent VI at the geometric midpoint of the link and assess the impact to data assimilation. We explore the impact of adding OI data to three baseline runs: one with only ionosonde data (*I*), one with ionosonde and Radio Occultation (RO) data (*IR*), and one with ionosonde, RO, and ground-based Total Electron Content (TEC) data (*IRG*). While it may be natural to assume that more data is always better for data assimilation, we find that there are locations and times when ingesting OI data with the quasi-midpoint formula does more harm than good. We present our findings and recommendations for best OI filtering practices.

1. Introduction

Oblique Ionograms (OIs) are powerful tools that measure group path delay beyond the localized view of vertical ionograms (VIs) along a specific propagation path between a transmitter and receiver that are separated across long (and sometimes inaccessible) distances. They can provide real-time information on ionospheric conditions including optimal operating frequencies for reliable HF communication, Maximum Usable Frequency (MUF), and Lowest Usable Frequency (LUF). They are more complex than VIs, as each frequency travels along a separate path making an inversion non-unique. OIs can reveal multi-hop propagation modes, sky-wave backscatter characteristics, and ionospheric disturbances affecting radio links, thereby solidifying their crucial role in optimizing radio communication and ionospheric research across extended regions [1, 2].

There are two primary methods to assimilate OI data. The first is to use iterative ray tracing to adjust the ionosphere along the raypath until it better matches the OI data. This method is used by the GPSII (GPS Ionospheric Inversion) assimilator and is quite computationally intensive [3]. The second is to assume spherical symmetry and transform the OI into the equivalent VI. This method is used by Orion Space Solutions's ionospheric data assimilator, Modern Modular Model for Space Data Assimilation (M3SDA). M3SDA can use either a 3DVar or Cyclic Extended Kalman Filter (EKF) algorithm to minimize the cost function. Unlike parameterized models like Boston College's RIPE and the U.S. Naval Research Laboratory's ANCHOR, M3SDA can model ionospheres which depart from Chapman or semi-Epstein profiles.

For the research proposed in this paper, we use M3SDA in EKF mode with a 0 second correlation time to turn off cycling of the covariance and state. This mode extends that Kalman filter to utilize non-linear observation operators and uses the Jacobian of the observation operators to find the tangent line approximation. We note that the EKF assumes that the state and measurement probability distributions are Gaussian. For highly nonlinear systems, this assumption may not hold, since distributions can sometimes be multimodal or skewed. In the case that the Gaussian assumption is violated, estimates provided by the EKF can be suboptimal.

2. An OSSE over CONUS

Orion has developed the OSSE Tool (OSSET) to enable rapid and robust analysis of observing systems through numerical experiments. OSSET is a validated and trusted tool that has been instrumental in evaluating the impact of various types of data for the Air Force and NASA [4]. OSSEs have three steps: (1) a truth model and observation system(s) are selected, and measurements are simulated; (2) the simulated measurements are ingested into an assimilative ionospheric model and an analysis is produced; and (3) user-selected metrics are computed for the background and the analysis to assess the improvement in the specification based on the ingested data. This process can be repeated as many times as desired for different locations, times, and types of data.

It is also essential to use a truth model with realistic small-scale variances to ensure accurate OSSE results. Orion developed and validated the Noisy Truth Model (NTM) to better replicate small-scale variabilities relevant to HF propagation metrics. The NTM builds on the smooth, physics-based TIE-GCM model by adding correlated noise [5], with correlations applied horizontally, vertically, and temporally. These correlations are informed by two years of mid-latitude ionosonde data, with noise parameters varying by season, solar activity, local time, and altitude.

The OSSEs performed for this study over the continental US (CONUS) followed 4 steps. First, OIs were simulated by homing rays (using PhaRLAP) of various frequencies and recording the group delays between transmission and receipt. Second, delays and frequencies were transformed to their equivalent vertical quantities using the quasi-midpoint formula. Third, equivalent delays and frequencies were converted to a bottom-side electron density profile (EDP) using the POLynomial Analysis (POLAN) program [6], with the relations found in Equations 1 and 2:

$$h_c = \frac{1}{2}\left(-B + \sqrt{B^2 - 4C}\right) \qquad (1)$$

Here, h_c is the equivalent delay for a vertical ionosonde at the midpoint; $B = 2R_E(1 - \cos\frac{D}{2R_E})$ relates the radius of Earth, R_E, and the range, D; and $C = 2R_E^2(1 - \cos\frac{D}{2R_E}) - \left(\frac{p}{2}\right)^2$ relates the radius of Earth, range, and group delay, p.

$$f_{vi} = f_{ob}\sqrt{1 - \left(\frac{R_E \cos\beta}{R_E + h_c}\right)^2} \qquad (2)$$

In Equation 2, f_{vi} is the equivalent frequency for a vertical ionosonde at the midpoint; f_{ob} is the frequency of the synthesized oblique traces; and β is the elevation angle at h_c, calculated above in Equation 1. The equivalent vertical ionogram is referred to as a 'retrieved' in Figure 1.

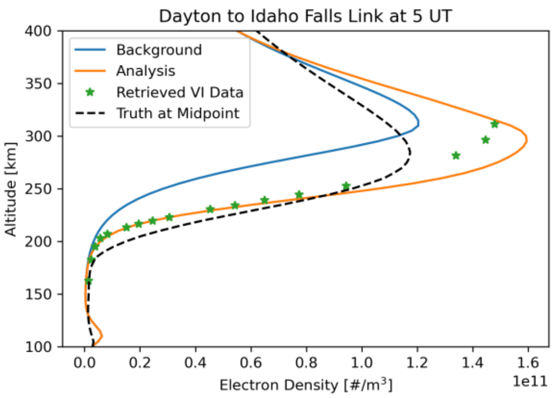

Figure 1. Sample assimilated EDPs resulting from the multi-step OSSE process.

Finally, EDPs were assimilated in M3SDA's EKF mode. The assimilated EDPs for the Dayton (Ohio) to Idaho Falls (Idaho) link can be found in Figure 1 above, where the green stars represent the data computed in the third step of the process delineated above. They deviate most from the dashed black line showing the truth at the midpoint, especially near the peak where the OI data drastically overshoots the truth. This difference shows the impact of the assumption of spherical symmetry used in the transform from OI to VI. While this difference can be small in some cases, for this link and several others, the data steers the analysis in the wrong direction, causing an enhancement in the F region, and showing that the retrieved VI does more harm than good.

3. Chosen Runs

We considered three baseline runs for our OSSEs for a full day, using foF2 as a metric: one with only ionosonde data (*Run I*); one with ionosonde and radio occultation (RO) data (*Run IR*); and another with ionosonde, RO, and ground-based Total Electron Content (TEC) data (*Run IRG*). For simplicity, we will discuss our analysis of Run I in this paper, though all three baseline runs will be presented. Two additional runs were performed for each baseline run, where either all oblique data were ingested (named, for example, Run I + All OIs) or some oblique data were ingested (named, for example, Run I + Some OIs). OI links were removed in the case that the haversine distance between the transmitter coordinates and the receiver coordinates was more than 1750 km. This was our choice for the threshold that constituted a 'long link' distance.

4. Results

We began our detailed analysis by mapping foF2 for each of the Truth (NTM), the Background (IRI), Run I, Run I + All OIs, and Run I + Some OIs (as seen in Figure 2). We find that truth fof2 is much lower than the IRI background on average. Next, we consider mean errors for the entire length of the run, as well as errors at each timestep. These are computed by subtracting the truth from all other models. We also find that all model runs perform better than IRI. Next, we introduce the 'improvement' metric, which is computed by subtracting the IRI errors from all assimilated models; the 'value' metric, which compares the runs with OIs to the baseline Run I; and the 'difference' metric, which directly compared the impact of ingesting some or all OIs.

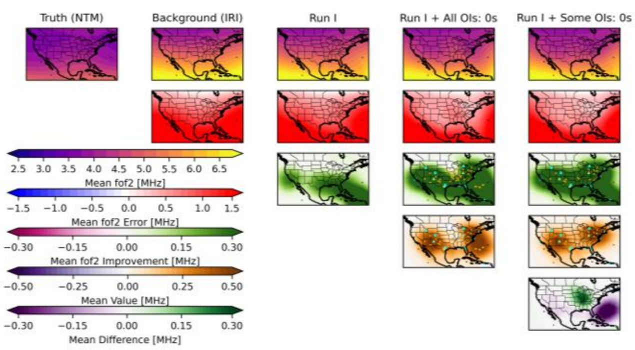

Figure 2. 'Stair-step' analysis of performance metrics for model performance of Run I averaged over a full day (04/01/2020).

The mean *value* and *difference* are shown in Figure 3. In the bottom right panel, we find our most interesting results: namely that there are places where ingesting OIs does more harm than good in terms of foF2 specification.

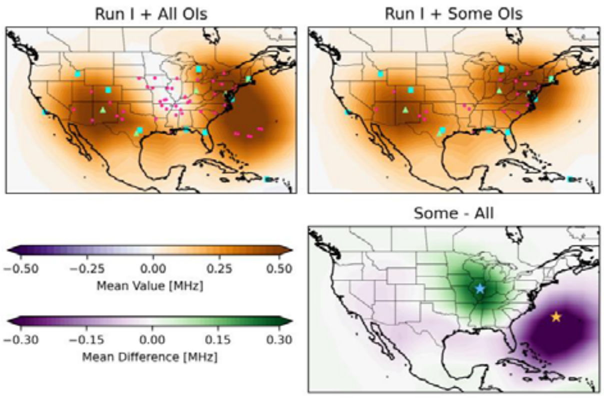

Figure 3. Mean *value* and *difference* metrics for foF2, comparing Run I with all OIs to the run with long links removed. In the upper two panels, blue squares represent VI locations, green triangles show hypothetical OI receivers, and the magenta dots mark OI midpoints. In the bottom panel, the blue and orange star represent locations for the case study found below in Figure 4.

Ingesting all OIs leads to an enhanced performance in regions like the Northeast and the Caribbean (dark orange regions in the top left panel and dark purple region in the bottom right panel). Whereas in the Midwest, where OI links tend to be long and oriented in the East-West direction, it is better, on average, to withhold long links (as evidenced by the green swath in the bottom right panel). This type of conditional performance is what we have dubbed a 'land for sea' trade. This is likely the case due to the strong horizontal gradients that impact their links, especially near dawn and dusk, violating the assumptions of the quasi-midpoint formula. When this assumption is violated, performance is impacted negatively.

We have also expanded this study to include an examination of the performance of different runs over all timesteps, and we found that on average, performance over the Midwest is worst at night and around the terminator. Meanwhile, performance over Mexico, for example, is worse later in the day.

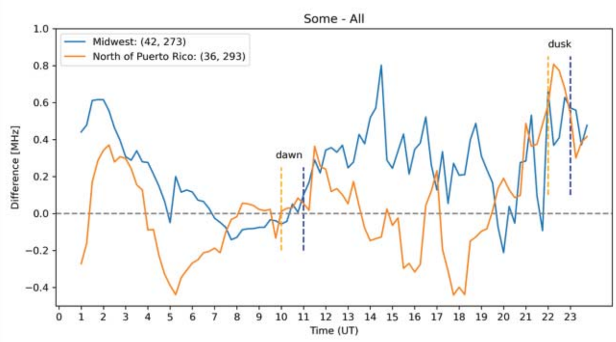

Figure 4. Case study of the time series of the *difference* metric for a location in the Midwest (blue) and another off the southeastern coast (orange). Dashed lines with corresponding colors to each location mark dawn and dusk.

To further explore regional temporal trends in model performance, we conducted a case study with two locations marked on the map of CONUS in the bottom panel of Figure 3, with one in the Midwest (near Chicago, IL), and another off the southeastern coast. In Figure 4, values above the horizontal dashed line indicate times when ingesting only shorter OI links leads to a better performance; whereas values below the horizontal dashed line indicate times when ingesting all links leads to the best performance. A quick pattern emerges for the blue point in the Midwest, where the curve resides above the dashed gray line throughout the day, indicating the positive effects of removing long links over this region.

Though such a clear pattern is not as clear for the location in orange, we note that there are times when it is clearly beneficial to ingest all OIs, further reiterating our findings of a 'land for sea' trade.

5. Conclusions

It is natural to think that using all oblique ionogram data available would lead to the best assimilative performance, but our study shows that this is not universally the case, especially when an assimilative model uses and Extended Kalman Filter. This is due to the inherent difficulties the EKF encounters when processing nonlinearities.

We have examined this phenomenon by filtering OI links based on length and found that long E-W links negatively impact performance. This is true for all three baseline runs with varying types of data ingested and is likely a product of the assumption of spherical symmetry used to assimilate oblique ionograms. These results, though impactful, may vary depending on the chosen method of ingesting OIs.

OI-filtering algorithms that factor in the horizontal gradient, such as the terminator, the Equatorial Ionization Anomaly (EIA), and the auroral ring, will prove incredibly helpful in accurate specification of the ionosphere through data assimilation. We plan to incorporate some of these filtering algorithms, to perform a more rigorous timestep analysis, and to add other types of M3SDA runs to our comparison, such as one with only ionosonde and RO data.

6. Acknowledgements

We acknowledge internal funding support from Arcfield Internal Research and Development. Some results in this paper were obtained using the HF propagation toolbox, PHaRLAP, created by Dr. Manuel Cervera, Defence Science and Technology Group, Australia (manuel.cervera@dsto.defence.gov.au). This toolbox is available by request from its author. PyLap, a Python-based interface to PHaRLAP, was also used (https://github.com/HamSCI/PyLap).

References

[1] FengJuan, S., XianRong, W., HongBo, Z. *et al.* Statistical and simulation study on the separation in junction frequencies between ordinary (O) and extraordinary (X) wave in oblique ionograms. *Earth Planets Space* **74**, 189 (2022). https://doi.org/10.1186/s40623-022-01755-7

[2] Rao, N. N. (1975), Analysis of discrete oblique ionogram traces in sweep-frequency sky-wave high resolution backscatter, *Radio Sci.*, 10(2), 149–153, doi:10.1029/RS010i002p00149.

[3] Fridman, S. V., L. J. Nickisch, M. Hausman, and G. Zunich (2016), Assimilative model for ionospheric dynamics employing delay, Doppler, and direction of arrival measurements from multiple HF channels, *Radio Sci.*, 51, 176–183, doi:10.1002/2015RS005890.

[4] Hughes, J., Collett, I., Crowley, G., Reynolds, A., & Azeem, I. (2024, May 15). Evaluating the impact of commercial radio occultation data using the observation system simulation experiment tool for Ionospheric Electron Density Specification. Frontiers. https://www.frontiersin.org/journals/astronomy-and-space-sciences/articles/10.3389/fspas.2024.1387941/full

[5] Hughes, J., Forsythe, V., Blay, R., Azeem, I., Crowley, G., Wilson, W. “J.”, et al. (2022). On constructing a realistic truth model using ionosonde data for Observation System Simulation Experiments. Radio Science, 57, e2022RS007508. https://doi.org/10.1029/2022RS007508

[6] Titheridge, J. E. (1985). “Ionogram analysis with the generalised program POLAN.” WORLD DATA CENTER A for Solar-Terrestrial Physics. https://www.ursi.org/files/CommissionWebsites/INAG/uag_93/uag93_ch1_5.pdf